ARISTOTLE UNIVERSITY OF THESSALONIKI
SCHOOL OF ELECTRICAL AND COMPUTER ENGINEERING
DEPARTMENT OF ELECTRONICS AND COMPUTER ENGINEERING

SYMPTOMATIC VS ASYMPTOMATIC PLAQUE CLASSIFICATION IN CAROTID ULTRASOUND

DIPLOMA THESIS
OF
NIKOLAOS G. GIAKOUMOGLOU

Supervisor: Anastasios Ntelopoulods

Thessaloniki, June 2021

Contents

Appendix A.   Textural Features

A.1   First-order statistics (FOS) or Statistical Features (SF)

Those features are resolution independent. Let $f(x, y)$ be the grayscale image. The first order histogram H_i is defined as

$$H_i = \frac{number\ of\ pixels\ with\ gray\ level\ i\ inside\ ROI}{total\ number\ of\ pixels\ in\ the\ ROI},$$

which is the empirical probability density function for single pixels. FOS/SF consists of the following parameters:

1. Mean

$$\mu = f_1 = \sum_i iH_i$$

2. Standar Deviation=Variance$^{1/2}$

$$\sigma = f_2 = \sqrt{\sum_i (i - \mu)^2 H_i}$$

3. Median

$$f_3 \ s.t. \sum_{i=0}^{f_3} H_i = 0.5$$

4. Mode

$$f_4 = \underset{i}{\mathrm{argmax}}\ \{H_i\}$$

5. Skewness

$$f_5 = \sum_i \left(\frac{i - \mu}{\sigma}\right)^3 H_i$$

6. Kurtosis

$$f_6 = \sum_i \left(\frac{i - \mu}{\sigma}\right)^4 H_i$$

7. Energy

$$f_7 = \sum_i H_i^2$$

8. Entropy

$$f_8 = -\sum_i H_i \ln [H_i]$$

9. Minimal Gray Level

$$f_9 = \min \{f(x, y)\}$$

10. Maximal Grey Level

$$f_{10} = \max \{f(x, y)\}$$

11. Coefficient of Variation

$$f_{11} = \frac{\sigma}{\mu}$$

12. 13. 14. 15. Percentiles (10,25,75,90)

$$f_n \ s.t. \sum_{i=0}^{f_n} H_i = c$$

where $(n, c) = (12, 0.1), (13, 0.25), (14, 0.75), (15, 0.9)$. Note that 50-Percentile is the median

16. Histogram Width

$$f_{16} = f_{15} - f_{12}$$

A.2 Gray Level Co-occurrence Matrix (GLCM) method or Spatial Gray Level Dependence Matrix (SGLDM) method

The spatial gray level dependence matrices as proposed by Haralick et al. are based on the estimation of the second-order joint conditional probability density functions, $\overline{p}(i, j; d, \theta)$. The $\overline{p}(i, j; d, \theta)$ is the probability that two pixels (k, l) and (m, n) with distance d in direction specified by the angle θ have intensities of gray level i and gray level j. The estimated values for these probability density functions will be denoted by $P(i, j, ; d, \theta)$. In a $N_1 \times N_2$ image, let $L_1 = \{0, 1, \dots, N_1 - 1\}$ be the horizontal spatial domain, $L_2 = \{0, 1, \dots, N_2 - 1\}$ be the vertical spatial domain, and $f(x, y)$ be the image intensity at pixel (x, y). Formally, for angles quantized at 45° intervals, the unnormalized probability density functions are defined by

$$P(i, j; d, 0^o) = \#\{((k, l), (m, n)) \in (L_1 \times L_2) \times (L_1 \times L_2): k - m = 0, |l - n| = d, f(k, l) = i, f(m, n) = j\}$$

$$P(i, j; d, 45^o) = \#\{((k, l), (m, n)) \in (L_1 \times L_2) \times (L_1 \times L_2): (k - m = d, |l - n| = d) \ or \ (k - m = -d, l - n = d), f(k, l) = i, f(m, n) = j\}$$

$$P(i, j; d, 90^o) = \#\{((k, l), (m, n)) \in (L_1 \times L_2) \times (L_1 \times L_2): |k - m| = d, l - n = 0, f(k, l) = i, f(m, n) = j\}$$

$$P(i, j; d, 45^o) = \#\{((k, l), (m, n)) \in (L_1 \times L_2) \times (L_1 \times L_2): (k - m = d, |l - n| = d) \ or \ (k - m = -d, l - n = -d), f(k, l) = i, f(m, n) = j\}$$

where # denotes the number of elements in the set.

Table A-1 GLCM notation

$p(i, j)$	$\dfrac{P(i, j)}{\sum_{i=0}^{N-1} \sum_{j=0}^{N-1} P(i, j)}$
N	number of gray levels
$p_x(i)$	$\sum_{j=0}^{N-1} p(i, j)$
$p_y(i)$	$\sum_{i=0}^{N-1} p(i, j)$

μ_x	$\sum_{i=0}^{N-1} i p_x(i)$
μ_y	$\sum_{j=0}^{N-1} j p_y(j)$
σ_x^2	$\sum_{i=0}^{N-1} (i - \mu_x)^2 p_x(i)$
σ_y^2	$\sum_{j=0}^{N-1} (j - \mu_y)^2 p_y(j)$
$p_{x+y}(k)$	$\sum_{i=0}^{N-1} \sum_{j=0, i+j=k}^{N-1} p(i,j)$
$p_{x-y}(k)$	$\sum_{i=0}^{N-1} \sum_{j=0, |i-j|=k}^{N-1} p(i,j)$
μ_{x+y}	$\sum_{k=1}^{2N-1} k p_{x+y}(k)$
μ_{x-y}	$\sum_{k=0}^{N-1} k p_{x-y}(k)$

Haralick et al. proposed the following texture measures that can be extracted from the spatial gray level dependence matrices:

1. Angular Second Moment= Energy^2

$$f_1 = \sum_{i=0}^{N-1} \sum_{i=0}^{N-1} p(i,j)^2$$

2. Contrast

$$f_2 = \sum_{i=0}^{N-1} n^2 \left\{ \sum_{i=0, |i-j|=n}^{N-1} \sum_{j=0}^{N-1} p(i,j) \right\}$$

3. Correlation

$$f_3 = \sum_{i=0}^{N-1} \sum_{j=0}^{N-1} \left(\frac{i - \mu_x}{\sigma_x} \right) \left(\frac{j - \mu_y}{\sigma_y} \right) p(i,j) = \frac{\sum_{i=0}^{N-1} \sum_{j=0}^{N-1} (ij) p(i,j) - \mu_x \mu_y}{\sigma_x \sigma_y}$$

4. Sum of Squares: Variance

$$f_4 = \sum_{i=0}^{N-1} \sum_{i=0}^{N-1} (i - \mu)^2 p(i,j)$$

5. Inverse Difference Moment (1st formula)/Homogeneity (2nd formula)

$$f_5 = \sum_{i=0}^{N-1} \sum_{i=0}^{N-1} \frac{p(i,j)}{1 + (i-j)^2} \text{ or } \sum_{i=0}^{N-1} \sum_{i=0}^{N-1} \frac{p(i,j)}{1 + |i-j|}$$

6. Sum Average

$$f_6 = \sum_{k=1}^{2N-1} k p_{x+y}(k)$$

7. Sum Variance

$$f_7 = \sum_{k=1}^{2N-1} (i - \mu_{x-y})^2 p_{x+y}(k)$$

8. Sum Entropy

$$f_8 = -\sum_{k=1}^{2N-1} p_{x+y}(k)\, ln[p_{x+y}(k)]$$

9. Entropy

$$f_9 = -\sum_{i=0}^{N-1}\sum_{i=0}^{N-1} p(i,j) log[p(i,j)]$$

10. Difference Variance

$$f_{10} = \sum_{k=0}^{N-1} (k - \mu_{x-y})^2 p_{x-y}(k)$$

11. Difference Entropy

$$f_{11} = -\sum_{k=0}^{N-1} p_{x-y}(ik) log\left[p_{x-y}(k)\right]$$

12. 13. Information Measures of Correlation

$$f_{12} = \frac{HXY - HXY1}{\max\{HX, HY\}}$$

$$f_{13} = (1 - \exp(-2.0(HXY2 - HXY])^{1/2}$$

where

$$HX = -\sum_{i=0}^{N-1} p_x(i) log[p_x(i)]$$

$$HY - \sum_{i=0}^{N-1} p_y(i) log[p_y(i)]$$

$$HXY - \sum_{i=0}^{N-1}\sum_{i=0}^{N-1} p(i,j) log[p(i,j)]$$

$$HXY1 = -\sum_{i=0}^{N-1}\sum_{i=0}^{N-1} p(i,j) log[p_x(i,j)Pp_y(i,j)]$$

$$HXY2 = -\sum_{i=0}^{N-1}\sum_{i=0}^{N-1} p(i,j) log[p_x(i,j)Pp_y(i,j)]$$

14. Maximal Correlation Coefficient

$$f_{14} = (Second\ largest\ Eigenvalue\ of\ Q)^{1/2}$$

where

$$Q(i,j) = \sum_{k=0}^{N-1} \frac{p(i,k)p(j,k)}{p_x(i)p_y(k)}$$

For a chosen distance d we have four angular SGLDM. Hence, we obtain a set of four values for each of the proceding measures. The mean and range of each of these measures, averaged over the four values, comprise the set of features which are used as input to the classifier.

A.3   Gray level difference statistics (GLDS) method

The GLDS algorithm uses first order statistics of local property values based on absolute differences between pairs of gray levels or of average gray levels in order to extract texture measures. Let $f(x, y)$ be the image intensity function and for any given displacement $\delta = (\Delta x, \Delta y)$, let $f_\delta(x, y) = |f(x, y) - f(x + \Delta x, y + \Delta y)|$. Let p_δ be the probability density of $f_d(x, y)$. If there are N gray levels, this has the form of an N-dimensional vector whose i^{th} component is the probability that $f_d(x, y)$ will have value i. The probability density p_δ can be easily computed by counting the number of times each value of $f_d(x, y)$ occurs, where Δx and Δy are integers. In a coarse texture, if the d is small, $f_d(x, y)$ will be small, i.e., the values of p_δ should be concentrated near $i = 0$. Conversely, in a fine texture, the values of p_δ should be more spread out. Thus, a good way to analyze texture coarseness would be to compute, for various magnitudes of δ, so memeasure of the spread of values in p_δ away from the origin. Such measures are the following

1. Homogeneity

$$f_1 = HOM = \sum_i \frac{p_\delta(i)}{i^2 + 1}$$

2. Contrast

$$f_2 = CON = \sum_i i^2 p_\delta(i)$$

3. Energy/ Angular Second Moment

$$f_3 = ASM = \sum_i p_\delta(i)^2$$

4. Entropy

$$f_4 = ENT = -\sum_i p_\delta(i) log[p_\delta(i)]$$

5. Mean

$$f_5 = MEAN = \sum_i i p_\delta(i)$$

A.4 Neighborhood gray tone difference matrix (NGTDM) method

NGTDM corresponds to visual properties of texture. Let $f(x, y)$ be the gray tone of a pixel at (x, y) having gray tone value i. Then the average gray tone over a neighborhood centered at, but excluding (x, y), can be found

$$A_i = A(x, y) = \frac{1}{W - 1} \sum_{x'=-d}^{d} \sum_{y'=-d}^{d} f(x + x', y + y')$$

where $(x', y') \neq (0,0)$, d specifies the neighborhood size and $W = (2d + 1)^2$. Then the ith entry in the NGTDM is

$$s(i) = \begin{cases} \sum |i - A_i|, for\ i \in N_i\ if\ N_i \neq 0 \\ 0, otherwise \end{cases}$$

where $\{N_i\}$ is the set of all pixels having gray tone i.

Table A-2 NGTDM notation

G_h	highest gray tone value present in the image
ε	a small number
$p_i = \dfrac{N_i}{n^2},\ n = N - 2d$	the probability of occurrence of gray tone value i in a $N \times N$ image
N_g	total number of different gray levels present in the image

The following textural features are defined as

1. Coarseness

$$f_1 = COS = \left[\varepsilon + \sum_{i=0}^{G_h} p_i s(i)\right]^{-1}$$

2. Contrast

$$f_2 = CON = \left[\frac{1}{N_g(N_g - 1)}\sum_{i=0}^{G_h}\sum_{j=0}^{G_h} p_i p_j (i - j)^2\right]\left[\frac{1}{n^2}\sum_{i=0}^{G_h} s(i)\right]$$

3. Busyness

$$f_3 = BUS = \frac{\left[\sum_{i=0}^{G_h} p_i s(i)\right]}{\left[\sum_{i=0}^{G_h} i p_i - j p_j\right]}, p_i \neq 0, p_j \neq 0$$

4. Complexity

$$f_4 = COM = \sum_{i=0}^{G_h}\sum_{j=0}^{G_h} \{(|i - j|)/(n^2(p_i + p_j))\}\{p_i s(i) + p_j s(j)\}$$
$$p_i \neq 0, p_j \neq 0$$

5. Strength

$$f_5 = STR = \left[\sum_{i=0}^{G_h}\sum_{j=0}^{G_h}(p_i + p_j)(i - j)^2\right]\Big/\left[\varepsilon + \sum_{i=0}^{G_h} s(i)\right], p_i \neq 0, p_j \neq 0$$

A.5 Statistical feature matrix (SFM) method

The statistical feature matrix measures the statistical properties of pixel pairs at several distances within an image which are used for statistical analysis. Let $f(x, y)$ be the intensity at point (x, y), and let $\delta = (\Delta x, \Delta y)$ represent the intersample spacing distance vector, where Δx and Δy are integers. The δ contrast, δ covariance, and δ dissimilarity are defined as

$$CON(\delta) = E\{[|f(x, y) - f(x + \Delta x, y + \Delta y)]^2\}$$
$$COV(\delta) = E\{[f(x, y) - \eta][f(x + \Delta x, y + \Delta y) - \eta]\}$$
$$DSS(\delta) = E\{[f(x, y) - f(x + \Delta x, y + \Delta y)]\}$$

where $E\{\}$ denotes the expectation operation and η is the average gray level of the image. A statistical feature matrix, (SFM) M_{sf}, is an $(L_r + 1) \times (2L_c + 1)$ matrix whose (i, j) element is the δ statistical feature of the image, where $\delta = (j - L_c, i)$ is an intersample spacing distance vector for $i = 0, 1, \ldots, L_r$, $j = 0, 1, \ldots, L_c$, and L_r, L_c are the constants which determine the maximum intersample spacing distance. In a similar way, the contrast

matrix (M_{con}), covariance matrix (M_{cov}), and dissimilarity matrix (M_{dss}) can be defined as the matrices whose (i, j) elements are the δ contrast, δ covariance, and δ dissimilarity, respectively. Based on the SFM, the following texture features can be computed:

1. Coarseness

$$f_1 = CRS = \frac{c}{\sum_{(i,j)\in N_r} \frac{DSS(i,j)}{n}}$$

   where c is a normalized factor, N_r is the set of displacement vectors defined as $N_r = \{(i,j): |i|, |j| < r\}$ and n is the number of elements in the set.

2. Contrast

$$f_2 = CON = \left[\sum_{(i,j)\in N_r} \frac{CON(i,j)}{4}\right]^{1/2}$$

3. Periodicity

$$f_3 = PER = \frac{\bar{M}_{dss} - M_{dss}(valley)}{\bar{M}_{dss}}$$

   where $\bar{M}_{dss}$ is the mean of all elements in M_{dss} and $M_{dss}(valley)$ is the deepest valley in the matrix.

4. Roughness

$$f_4 = RGH = \frac{D_f^{(h)} + D_f^{(v)}}{2}$$

   Where D_f is the fractal dimension (see Fractal Dimension Texture Analysis (FDTA)) in horizontal and vertical dimensions. $D_f = 3 - H$ and $E\{-\Delta I\} = k(\delta)^H$ where H can be estimated from the dissimilarity matrix since the $(i, j + L_c)$ element of the matrix is $E\{-\Delta I\}$ with $\delta = (j, i)$.

A.6 Law's texture energy (LTE) method (TEM)

Law's texture energy measures are derived from three simple vectors of length 3, $L3 = (1,2,1), E3 = (-1,0,1), and\ S3 = (-1,2,-1)$, which represent the one-dimensional operations of center-weighted local averaging, symmetric first differencing for edge detection, and second differencing for spot detection. If these vectors are convolved with themselves, new vectors of length 5, $L5 = (1,4,6,4,1), E5 = (-1,-2,0,2,1)\ and\ S5 = (-1,0,2,0,-1)$ are obtained. By further self-convolution, new vectors of length 7, $L7 = (1,6,15,20,15,6,1), E7 = (-1,-4,-5,0,5,4,1)\ and\ S7 = (-1,-2,1,4,1,1,-2,-1)$ are obtained, where $L7$ again performs local averaging, $E7$ acts as edge detector, and $S7$ acts as spot detector. If the column vectors of length l are multiplied by row vectors of the same length, Laws $l \times l$ masks are obtained. The following combinations are used to obtain the masks (for $l = 7$):

$$LL = L7^T L7$$
$$LE = L7^T E7$$
$$LS = L7^T S7$$
$$EL = E7^T L7$$
$$EE = E7^T E7$$
$$ES = E7^T S7$$

$$SL = S7^T L7$$
$$SE = S7^T E7$$
$$SS = S7^T S7$$

In order to extract texture features from an image, these masks are convoluted with the image, and the statistics (e.g., energy) of the resulting image are used to describe texture. The following texture features were extracted:

1. LL- texture energy from LL kernel
2. EE- texture energy from EE kernel
3. SS- texture energy from SS kernel
4. LE- average texture energy from LE and EL kernels $LE = (LE + EL)/2$
5. ES- average texture energy from ES and SE kernels $ES = (ES + SE)/2$
6. LS- average texture energy from LS and SL kernels $LS = (LS + SL)/2$

The averaging of matched pairs of energy measures gives rotational invariance.

A.7   Fractal Dimension Texture Analysis (FDTA)

FDTA describe the roughness of nature surfaces. It considers naturally occurring surfaces as the end result of random walks. Such random walks are basic physical processes in our universe. An important parameter to represent a fractal dimension is the fractal dimension D_f estimated theoretically by the equation

$$E(\Delta I^2) = c(\Delta r)^{6-2D_f}$$

where $E(\cdot)$ denotes the expectation operator, ΔI is the intensity difference between two pixels, c is a constant, and Dr is the distance between two pixels. A simpler method is to estimate the H parameter (Hurst coefficient) from

$$E(|\Delta I|) = k(\Delta r)^H$$

where $k = E(|\Delta I|)_{\Delta r=1}$. By applying the log function the following is obtained

$$logE(|\Delta I|) = logk + Hlog(\Delta r)$$

From the above equation, the H parameter can be estimated and the fractal dimension D_f can be computed from the relationship

$$D_f = 3 - H$$

A smooth surface is described by a small value of the fractal dimension D_f (large value of the parameter H) where the reverse applies for a rough surface. Given an $M \times M$ image, the intensity difference vector is defined as

$$IDV = [id(1), id(2), ..., id(s)]$$

where s is the maximum possible scale, $id(k)$ is the average of the absolute intensity difference of all pixel pairs with vertical or horizontal distance k. The value of the parameter H can be obtained by using least squares linear regression to estimate the slope of the curve of $id(k)$ versus k in log–log scales.

If the image is seen under different resolutions, then the multiresolution fractal (MF) feature vector is defined as

$$MF = (H^m, H^{m-1}, ..., H^{m-n+1})$$

where $M = 2^m$ is the size of the original image, H^k is the H parameter estimated from image I^k, and n is the number of resolutions chosen. The multiresolution fractal (MF) feature vector describes also the lacunarity of the image. It can be used for the separation

of textures with the same fractal dimension D_f by considering all but the first components of the MF vectors.

A.8 Gray Level Run Length Matrix (GLRLM)

A gray level run is a set of consecutive, collinear picture points having the same gray level value. The length of the run is the number of picture points in the run. For a given picture, we can compute a gray level run length matrix for runs having any given direction θ. Often the direction θ is set as $0, 45, 90, 135^o$. The matrix element $p_\theta(i,j)$ specifies the number of times that the picture contains a run of length j, in the given direction, consisting of points having gray level i (or lying in gray level range i). Computation of these matrices is very simple. The number of calculations is directly proportional to the number of points in the picture. Also, the entire picture need not reside in core. Only two rows of picture values are needed at any one time to compute the matrices. To obtain numerical texture measures from the matrices, we can compute functions analogous to those used by Haralick for gray level co-occurrence matrices.

Table A-3 GLRLM notation

$p_\theta(i,j)$	The $(i,j)^{\text{th}}$ entry in the given run length matrix for direction θ
N_g	Number of gray levels in the image
N_r	Number of different run length that occur (so the matrix is $N_g \times N_r$)
N_z	$\sum_{i=1}^{N_g} \sum_{j=1}^{N_r} p_\theta(i,j)$
N_p	The number of voxels in the image

The RUNL features are the following:
1. Short Run Emphasis

$$f_1 = \frac{\sum_{i=0}^{N_g-1} \sum_{j=0}^{N_r-1} \frac{p_\theta(i,j)}{j^2}}{N_z}$$

2. Long Run Emphasis

$$f_2 = \frac{\sum_{i=0}^{N_g-1} \sum_{j=0}^{N_r-1} j^2 p_\theta(i,j)}{N_z}$$

3. Gray Level Non-Uniformity/Gray Level Distribution

$$f_3 = \frac{\sum_{i=0}^{N_g-1} \left(\sum_{j=0}^{N_r-1} p_\theta(i,j)\right)^2}{N_z}$$

4. Run Length Non-Uniformity/Run Length Distribution

$$f_4 = \frac{\sum_{j=0}^{N_g-1} \left(\sum_{i=0}^{N_r-1} p_\theta(i,j)\right)^2}{N_z}$$

5. Run Percentage

$$f_5 = \frac{N_z}{N_p}$$

6. Low Gray Level Run Emphasis

$$f_6 = \frac{\sum_{i=0}^{N_g-1} \sum_{j=0}^{N_r-1} \frac{p_\theta(i,j)}{i^2}}{N_z}$$

7. High Gray Level Run Emphasis

$$f_7 = \frac{\sum_{i=0}^{N_g-1} \sum_{j=0}^{N_r-1} p_\theta(i,j)i^2}{N_z}$$

8. Short Low Gray Level Emphasis

$$f_8 = \frac{\sum_{i=0}^{N_g-1} \sum_{j=0}^{N_r-1} \frac{p_\theta(i,j)}{i^2 j^2}}{N_z}$$

9. Short Run High Gray Level Emhpasis

$$f_9 = \frac{\sum_{i=0}^{N_g-1} \sum_{j=0}^{N_r-1} \frac{p_\theta(i,j)}{j^2}}{N_z}$$

10. Long Run Low Gray Level Emphasis

$$f_{10} = \frac{\sum_{i=0}^{N_g-1} \sum_{j=0}^{N_r-1} \frac{p_\theta(i,j)}{i^2}}{N_z}$$

11. Long Run High Gray Level Emphasis

$$f_{11} = \frac{\sum_{i=1}^{N_g-1} \sum_{j=1}^{N_r-1} p_\theta(i,j)i^2 j^2}{N_z}$$

A.9 Fourier power spectrum (FPS)

The Fourier transform of a picture $f(x,y)$ is defined by

$$F(u,v) = \int_{-\infty}^{\infty} \int_{-\infty}^{\infty} e^{-2\pi i(ux+vy)} f(x,y)dxdy$$

and the Fourier power spectrum, is $|F|^2 = FF^*$ (where $*$ denontes the complex conjugate).

It is well known that the radial distribution of values in $|F|^2$ is sensitive to texture coarseness in f. A coarse texture will have high values of $|F|^2$ concentrated near the origin while in a fine texture the values of $|F|^2$ will be more spread out. Thus if one wishes to analyze texture coarsenesss, a set of features that should e usefull are the averages of $|F|^2$ taken over a ring-shaped regions centred at the origin i.e. features of the form

$$\varphi_r = \int_0^{2\pi} |F(r,\theta)|^2 \, d\theta$$

for various values of r, the ring radius.

Similarly, it is well known that the angular distribution of values in $|F|^2$ is sensitive to the directionality of the texture in f. A texture with many edges or lines in a given

direction θ will have high values of $|F|^2$ concentrated around the perpendicular direction $\theta + \left(\frac{\pi}{2}\right)$, while in a nondirectional texture, $|F|^2$ should also be nondirectional.Thus a good set of features for analyzing texture direcdtionality should be the averages of $|F|^2$ taken over a wedge-shaped regions entered at the origin, i.e., features of the form

$$\varphi_\theta == \int\limits_0^\infty |F(r,\theta)|^2 \, d\theta$$

for various values of θ, the wedge slope.

For $N \times N$ digital pictures, instead off the continuous Fourier transform defined above, one uses the discrete transfrom defined by

$$F(u,v) = \frac{1}{N^2} \sum_{i,j=0}^{N-1} f(i,j)e^{-2\pi\sqrt{-1}(iu+jv)}$$

where $0 \leq u$ and $v \leq N - 1$. This transofrm, however treats the input picture $f(x,y)$ as periodic. If, in fact, it is not, the transform is affected by the discontinuites that exist between one edge of f and the opposite edge. These have the effect of introducing spurious horizontal and vertical directionalities, so that high alues are present in $|F|^2$ akibg tge u and v axes.

The standard set of texture features based on a ring-shaped samples of the discrete Fourier power spectrum are of the form

$$\varphi_{r_1,r_2} = \sum_{r_1 \leq u^2+v^2 \leq r_2} |F(u,v)|^2$$

for various values of the inner and outer ring radii r_1 and r_2. Similarly, the features based on a wedge-shaped samples are of the form

$$\varphi_{\theta_{1.\theta_2}} = \sum_{\theta_1 \leq \tan^{-1}\left(\frac{v}{u}\right) \leq \theta_2} |F(u,v)|^2$$

Note that in this last set of features, the "DC value" $(u,v) = (0,0)$ has been omitted, since it is common to all the wedges.

A.10 Shape parameters

Shape parameters consists of the following parameters:
1. X-coordinate maximum length
2. Y-coordinate maximum length
3. area
4. perimeter
5. perimeter^2/area

A.11 High Order Spectra (HOS) on Radon Transform

Radon transform and Hough transform have received more attention in image processing recently. They transform two dimensional images with lines into a domain of possible line parameters, where each line in the image will give a peak positioned at the corresponding line parameters. Hence, the lines of the images are transformed into the

points in the Radon domain. An equation of the line can be expressed as: $\rho = x \cdot \cos\theta + y \cdot \sin\theta$, where θ is the small angle and ρ is the small distance to the origin of the coordinate system. Given a function $f(x, y)$, Radon transform is defined as:

$$R(\rho, \theta) = \int_{-\infty}^{\infty} f(\rho \cdot \cos\theta - s \cdot \sin\theta, \rho \cdot \sin\theta + s \cdot \cos\theta)ds$$

This equation describes the integral along a line s through the image, where ρ is the distance of the line from the origin and θ is the angle from the horizontal. So, radon transform converts 2D signal into the 1D parallel beam projections, at various angles, θ.

High Order Spectra are spectral components of higher moments. The bispectrum $B(f_1, f_2)$, of a signal is the Fourier transform (FT) of the third order correlation of the signal (also known as the third order cumulant function). It is given by

$$B(f_1, f_2) = E\{X(f_1)X(f_2)X^*(f_1 + f_2)\}$$

where $X(f)$ is the FT of the signal $x[n]$, $E[\cdot]$ stands for the expectation operation and $X^*(f_1 + f_2)$ denotes the complex conjugate of $X(f_1 + f_2)$. The frequency f may be normalized by the Nyquist frequency to be between 0 and 1. The bispectrum, is a complex-valued function of two frequencies. The bispectrum which is the product of three Fourier coefficients, exhibits symmetry and was computed in the non-redundant region. This is termed as Ω, the principal domain or the nonredundant region.

The extracted feature is the entropy 1 (P_1)

$$Entropy1: P_1 = -\sum_i p_i \log(p_i)$$

where

$$p_i = \frac{|B(f_1, f_2)|}{\sum_\Omega |B(f_1, f_2)|}$$

A.12 Local Binary Pattern (LPB)

LBP, a robust and efficient texture descriptor, was first presented by Ojala et al. (1996, 2002). The LBP feature vector, in its simplest form, is determined using the following method: A circular neighborhood is considered around a pixel. P points are chosen on the circumference of the circle with radius R such that they are all equidistant from the center pixel. Let g_c be the gray value of the center pixel and $g_p, p = 0, ..., P - 1$, corresponds to the gray values of the P points. These P points are converted into a circular bit-stream of 0s and 1s according to whether the gray value of the pixel is less than or greater than the gray value of the center pixel. Ojala et al. (2002) introduced the concept of uniformity in texture analysis. The uniform fundamental patterns have a uniform circular structure that contains very few spatial transitions U (number of spatial bitwise 0/1 transitions). In this work, a rotation invariant measure called $LBP_{P,R}$ using uniformity measure U was calculated. Only patterns with $U \leq 2$ were assigned the LBP code i.e., if the number of bittransitions in the circular bit-stream is less than or equal to 2, the center pixel was labelled as uniform.

$$LBP_{P,R}(x) = \begin{cases} \sum_{p=0}^{P-1} s(g_p - g_c), & if \ U(x) \leq 2 \\ P + 1, & otherwise \end{cases}$$

where
$$s(x) = \begin{cases} x, & x \geq 0 \\ 0, & x < 0 \end{cases}$$

Multiscale analysis of the image using LBP is done by choosing circles with various radii around the center pixels and, thus, constructing separate LBP image for each scale. Energy and entropy of the LBP image, constructed over different scales ($R = 1,2,3$ with corresponding pixel count $P = 8,16,24$ respectively) were used as feature descriptors.

A.13 Gray Level Size Zone Matrix (GLSZM)

A Gray Level Size Zone (GLSZM) quantifies gray level zones in an image. A gray level zone is defined as the number of connected voxels that share the same gray level intensity. A voxel is considered connected if the distance is 1 according to the infinity norm (26-connected region in a 3D, 8-connected region in 2D). In a gray level size zone matrix $P(i,j)$ the $(i,j)^{th}$ element equals the number of zones with gray level i and size j appear in image. Contrary to GLCM and GLRLM, the GLSZM is rotation independent, with only one matrix calculated for all directions in the ROI.

Table A-4 GLSZM notation

N_g	Number of discreet intensity values
N_s	Number of discreet zones
N_p	Number of voxels
$N_z = \sum_{i=0}^{N_g-1} \sum_{j=0}^{N_s-1} P(i,j), 1 \leq N_z \leq N_p$	Number of zones in the ROI
$P(i,j)$	Size zone matrix
$p(i,j) = \dfrac{P(i,j)}{N_z}$	Normalized size zone matrix

The following features can be calculated
1. Small Zone Emphasis (SZE) or Small Area Emphasis (SAE)
$$f_1 = \sum_{i=0}^{N_g-1} \sum_{j=0}^{N_s-1} \frac{p(i,j)}{j^2}$$
2. Large Zone Emphasis (LZE) or Large Area Emphasis (LAE)
$$f_2 = \sum_{i=0}^{N_g-1} \sum_{j=0}^{N_s-1} p(i,j)j^2$$
3. Gray-Level Non-Uniformity (GLN)
$$f_3 = \frac{\sum_{i=0}^{N_g-1}\left(\sum_{j=0}^{N_s-1} P(i,j)\right)^2}{N_z} \quad or \quad \frac{\sum_{i=0}^{N_g-1}\left(\sum_{j=0}^{N_s-1} P(i,j)\right)^2}{N_z^2}$$
4. Zone-Size Nonuniformity(ZSN)

$$f_4 = \frac{\sum_{j=0}^{N_S-1}\left(\sum_{i=0}^{N_g-1}P(i,j)\right)^2}{N_z} \quad or \quad \frac{\sum_{j=0}^{N_S-1}\left(\sum_{i=0}^{N_g-1}P(i,j)\right)^2}{N_z^2}$$

5. Zone Percentage (ZP)

$$f_5 = \frac{N_z}{N_p}$$

6. Low Gray-Level Zone Emphasis (LGLZE)

$$f_6 = \sum_{i=0}^{N_g-1}\sum_{j=0}^{N_s-1}\frac{p(i,j)}{i^2}$$

7. High Gray-Level Zone Emphasis (HGLZE)

$$f_7 = \sum_{i=0}^{N_g-1}\sum_{j=0}^{N_s-1}p(i,j)i^2$$

8. Small Zone Low Gray-Level Emphasis (SZLGLE) or Small Area Low Gray-Level Emphasis (SALGLE)

$$f_8 = \sum_{i=0}^{N_g-1}\sum_{j=0}^{N_s-1}\frac{p(i,j)}{i^2 j^2}$$

9. Small Zone High Gray-Level Emphasis (SZHGLE) or Small Area High Gray-Level Emphasis (SAHGLE)

$$f_9 = \sum_{i=0}^{N_g-1}\sum_{j=0}^{N_s-1}\frac{p(i,j)i^2}{j^2}$$

10. Large Zone Low Gray-Level Empasis (LZLGLE) or Large Area Low Gray-Level Emphasis (LALGLE)

$$f_{10} = \sum_{i=0}^{N_g-1}\sum_{j=0}^{N_s-1}\frac{p(i,j)j^2}{i^2}$$

11. Large Zone High Gray-Level Emphasis (LZHGLE) or Large Area High Gray Level Emphasis (LAHGLE)

$$f_{11} = \sum_{i=0}^{N_g-1}\sum_{j=0}^{N_s-1}p(i,j)i^2 j^2$$

12. Gray-Level Variance (GLV)

$$f_{12} = \sum_{i=0}^{N_g-1}\sum_{j=0}^{N_s-1}p(i,j)(i-\mu)^2$$

$$\mu = \sum_{i=0}^{N_g-1}\sum_{j=0}^{N_s-1}p(i,j)i$$

13. Zone-Size Variance (ZSV)

$$f_{13} = \sum_{i=0}^{N_g-1} \sum_{j=0}^{N_s-1} p(i,j)(j-\mu)^2$$

$$\mu = \sum_{i=0}^{N_g-1} \sum_{j=0}^{N_s-1} p(i,j)j$$

14. Zone-Size Etropy (ZSE)

$$f_{14} = -\sum_{i=0}^{N_g-1} \sum_{j=0}^{N_s-1} p(i,j) \log_2(p(i,j) + \varepsilon)$$

ε is an arbitrarily small positive number

Appendix B.   Morhpological Features

B.1   Multilevel Binary Morhpological Analysis

In multilevel binary morphological analysis, the authors are interested in extracting different plaque components and investigating their geometric properties. They begin by generating three binary images by thresholding

$$L = \{(x,y) \ s.t. \ f(x,y) < 25\}$$
$$M = \{(x,y) \ s.t. \ 25 \leq f(x,y) \leq 50\}$$
$$H = \{(x,y) \ s.t. \ f(x,y) > 50\}$$

Here, binary image outputs are represented as sets of image coordinates where image intensity meets the threshold criteria. Overall, this multilevel decomposition is closely related to a three-level quantization of the original image intensity. To see this, note that the authors can simply assign quantization levels to each of the pixels in L, M, H and then use them to provide an approximate reconstruction of the original image. In L, the authors want to extract dark image regions representing blood, thrombus, lipid, or hemorrhage. Similarly, in H, the authors want to extract the collagen and calcified components of the plaque, while in M, the authors want to extract image components that fall between the two. Thus, to decide the threshold levels of (5), the authors varied the threshold levels so as to extract the desired components from the plaques. In the following discussion, the symbol X will be used to denote any one of the three binary images L, M, H.

The structural element, also known as pattern or kernel is defined as the set

$$B = \{(-1,0), (0,0), (1,0), (0,-1), (0,1)\} \subseteq Z^2$$

The two basic operators in the area of mathematical morphology is erosion and dilation. The basic effect of the erosion on a binary image is to erode away the boundaries of regions of foreground pixels (i.e. white pixels, typically). Thus areas of foreground pixels shrink in size, and holes within those areas become larger. Erosion is defined as

$$X \ominus B = \bigcup_{p \in B} X - p = \{a : B + a \subseteq X\}$$

The basic effect of the dilation on a binary image is to gradually enlarge the boundaries of regions of foreground pixels (*i.e.* white pixels, typically). Thus areas of foreground pixels grow in size while holes within those regions become smaller. Dilation is defined as

$$X \oplus B = \bigcup_{p \in B} X + p = \{a + b : a \in X \ and \ b \in B\}$$

The define the n-fold expansion of B also known as n-fold Minkowski addition of B with itself as

$$nB = \begin{cases} \{(0,0)\}, n = 0 \\ \underbrace{B \oplus B \oplus \ldots \oplus B}_{n-1 \ dilations} \ n > 1 \end{cases}$$

Opening and closing are two important operators from mathematical morphology. They are both derived from the fundamental operations of erosion and dilation. The basic effect of an opening is somewhat like erosion in that it tends to remove some of the foreground (bright) pixels from the edges of regions of foreground pixels. However it is less destructive

than erosion in general. The effect of the opening is to preserve foreground regions that have a similar shape to this structuring element, or that can completely contain the structuring element, while eliminating all other regions of foreground pixels. Opening is defined as an erosion followed by a dilation:

$$X \circ B = (X \ominus B) \oplus B$$

Closing is similar in some ways to dilation in that it tends to enlarge the boundaries of foreground (bright) regions in an image (and shrink background color holes in such regions), but it is less destructive of the original boundary shape. The effect of the closing is to preserve background regions that have a similar shape to this structuring element, or that can completely contain the structuring element, while eliminating all other regions of background pixels. Closing is defined as a dilation followed by an erosion:

$$X \bullet B = (X \oplus B) \ominus B$$

Opening and closing are idempotent, i.e. their successive applications do not change further the previously transformed result

$$X \circ B = (X \circ B) \circ B$$
$$X \circ B = (X \bullet B) \bullet B$$

We define as a multiscale opening of X by B also known as set-processing (SP) opening at scale $n = 0,1,2,..$, the opening

$$X \circ nB = (X \ominus nB) \oplus nB$$

A dual multiscale filter is the closing of X by nB or set-processing (SP) closing

$$X \bullet nB = (X \oplus nB) \ominus nB$$

The SP opening can be implemented more efficiently as

$$X \circ nB = \left[\underbrace{(X \ominus B) \ominus B \ominus ... \ominus B}_{n\ times} \right] \left[\underbrace{\oplus B \oplus B \oplus ... \oplus B}_{n\ times} \right]$$

The set difference images can be formed as

$$d_0(X;B) = X - X \circ B$$
$$d_1(X;B) = X \circ B - X \circ 2B$$
$$...$$
$$d_{n-1}(X;B) = X \circ (n-1)B - X \circ nB$$

The pattern spectrum is defined as the function

$$PS_X(n,B) = A[X \circ nB] - A[X \circ (n+1)B] = A[d_n(X;B)], \qquad n \geq 0$$

hence the discrete pattern spectrum can be obtained via a forward area difference. A probability density function (pdf) measure is considered defined as

$$pdf_X(n,B) = \frac{A(PS_x(n,B))}{A(X)}, for\ n > 0$$

Given the pdf-measure, the cumulative distribution function (cdf) can also be constructed using

$$cdf_X(n,B) = \begin{cases} 0, n = 0 \\ \sum_{r=0}^{n-1} pdf_X(n,B), r+1 \geq n > 0 \end{cases}$$

B.2   Gray Scale Morhpological Analysis

Similarly we henceforth represent graytone images by functions; filters whose inputs and outputs are functions (multilevel signals) are called Function-Processing (FP) filters. Let $f(x,y)$ be a finite support graytone image function on Z^2, and let $g(x,y)$ be a fixed graytone pattern. In the context of morphology, g is called function structuring element.

The mathematical definition for grayscale erosion and dilation is identical except in the way in which the set of coordinates associated with the input image is derived. The erosion and the dilation of f by g are respectively the functions

$$(f \ominus g)(x,y) = \min_{(i,j)}\{f(x+i, y+j) - g(i,j)\}$$

$$(f \oplus g)(x,y) = \max_{(i,j)}\{f(x+i, y+j) - g(i,j)\}$$

Thus, the opening and the closing of f by g are respectively the functions

$$f \circ g = (f \ominus g) \oplus g$$

$$f \bullet g = (f \oplus g) \ominus g$$

We define the multiscale function-processing (FP) opening of f by g at scale $n = 0,1,2,....$ as the function

$$f \circ ng = (f \ominus ng) \oplus ng$$

Likewise, we define the multiscale function-processing (FP) closing of f by g as the function

$$f \bullet ng = (f \oplus ng) \ominus ng$$

We can implement multiscale FP opening more efficient as

$$f \circ ng = \left[\underbrace{(f \ominus g) \ominus g \ominus ... \ominus g}_{n \ times} \right] \left[\underbrace{\oplus g \oplus g \oplus ... \oplus g}_{n \ times} \right]$$

Likewise for $f \bullet ng$. We define the pattern spectrum of f relative to a discrete graytone pattern g the function

$$PS_f(n,g) = A[f \circ ng - f \circ (n+1)g], \qquad 0 \le n \le N$$

where $A(f) = \sum_{(x,y)} f(x,y)$ and $(a-b)(x) = a(x) - b(x)$ denotes the pointwise algebraic difference between functions $a(x)$ and $b(x)$. N is the maximum positive size n such that $f \ominus ng$ is not all $-\infty$. A probability density function (pdf) measure is defined as

$$pdf_f(n,B) = \frac{A(PS_x(n,B))}{A(X)}$$

Given the pdf-measure, the cumulative distribution function (cdf) can also be constructed using

$$cdf_f(n,B) = \begin{cases} 0, n = 0 \\ \sum_{r=0}^{n-1} pdf_X(n,B), r+1 \ge n > 0 \end{cases}$$

Appendix C.   Histogram Features

C.1   Histogram

The grey level histogram of the ROI of the plaque image is computed for 32 equal width bins and used as an additional feature set. Histogram despite its simplicity provides a good description of the plaque structure.

C.2   Multi-region Histogram

Three equidistant ROIs were identified by eroding the plaque image outline by a factor based on the plaque size. The histogram was computed for each one of the three regions as described above and the 96 values comprised the new feature vector. This feature was computed in order to investigate whether the distribution of the plaque structure in equidistant ROIs has a diagnostic value and more specifically if the structure of the outer region of the plaque is critical whether the plaque will rupture or not.

C.3   Correlogram

Correlograms are histograms, which measure not only statistics about the features of the image, but also consider the spatial distribution of these features. In this work two correlograms were implemented for the ROI of the plaque image:

(i)   based on the distance of the distribution of the pixels' gray level values from the center of the image, and

(ii)   based on their angle of distribution.

For each pixel the distance and the angle from the image center was calculated and for all pixels with the same distance or angle their histograms were computed. In order to make the comparison between images of different sizes feasible, the distance correlograms were normalized into 32 possible distances from the center by dividing the calculated distances with $maximum\_distance/32$. The angle of the correlogram was allowed to vary among 32 possible values starting from the left middle of the image and moving clockwise. The resulting correlograms were matrices 32×32 (gray level values over 32 were set to be the white area surrounding the region of interest and were not consider for the calculation of the features).

Appendix D.   Multi-scale Features

D.1   Discrete Wavelet Transform (DWT)

The DWT of a signal x[n] is defined as its inner productwith a family of functions, $\phi_{j,k}(t)$ and $\psi_{j,k}(t)$, which form an orthonormal set of vectors, a combination of which can completely define the signal, and hence, allow its analysis in many resolution levels j.

$$\varphi_{j,k}(t) = 2^{\frac{j}{2}} \cdot \varphi(2^j t - k)$$

$$\psi_{j,k}(t) = 2^{\frac{j}{2}} \cdot \psi(2^j t - k)$$

The functions $\phi_{j,k}(t)$ and $\psi_{j,k}(t)$, consist of versions of the prototype scaling $\varphi(t)$, and wavelet $\psi(t)$ functions, discretized at level j and at translation k. However, for the implementation of the DWT, only the coefficients of two half-band filters: a low-pass $h(k)$ and a high-pass $g(k) = (-1)^k h(1 - k)$ filter, are required, which satisfy the following conditions:

$$\varphi_{j+1,0}(t) = \sum_k h[k]\varphi_{j,k}$$

$$\psi_{j+1,0}(t) = \sum_k g[k]\psi_{j,k}$$

Hence, the DWT is defined as follows:

$$A_{j+1,n} = \sum_k A_{j,k} \cdot h_j[k - 2n]$$

$$D_{j+1,n} = \sum_k D_{j,k} \cdot g_j[k - 2n]$$

where $A_{j,n}$ and $D_{j,n}$ are known as the approximation and detail coefficients, respectively, at level j and location n. The outputs $A_{j,n}$ and $D_{j,n}$ of the convolution are downsampled by two for every level of analysis, where the time resolution is halved and the frequency resolution is doubled.

For images, i.e., 2-D signals, the 2-D DWT can be used. This consists of a DWT on the rows of the image and a DWT on the columns of the resulting image. The result of each DWT is followed by downsampling on the columns and rows, respectively. The decomposition of the image yields four subimages for every level. Each approximation subimage (A_j) is decomposed into four subimages $[A_{j+1}, Dh_{j+1}, Dv_{j+1}, Dd_{j+1}]$ according to the previously described scheme. Each detail subimage is the result of a convolution with two half-band filters: a low-pass and a high-pass for Dh_j , a highpass and a low-pass for Dv_j , and two high-pass filters for Dd_j .
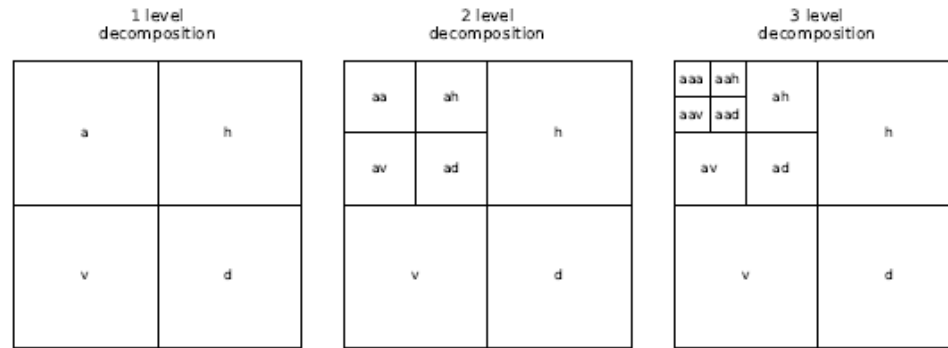
Figure D-1 DWT decomposition

D.2   Stationary Wavelet Transform (SWT)

The 2-D SWT is similar to the 2-D DWT, but no downsampling is performed. Instead, upsampling of the low-pass and high-pass filters is carried out. The main advantage of SWT over DWT is its shift invariance property.However, it is nonorthogonal and highly redundant, and hence, computationally expensive.

D.3   Wavelet Packets (WP)

The 2-D WP decomposition is a simple modification of the 2-D DWT, which offers a richer space-frequency representation. The first level of analysis is the same as that of the 2-D DWT. The second, as well as all subsequent levels of analysis consist of decomposing every subimage, rather than only the approximation subimage, into four new subimages.

D.4   Gabor Transform (GT)

The GT of an image consists in convolving that image with the Gabor function, i.e., a sinusoidal plane wave of a certain frequency and orientation modulated by a Gaussian envelope. Frequency and orientation representations of Gabor filters are similar to those of the human visual system, rendering them appropriate for texture segmentation and classification.

D.5   Multiresolution Feature Extraction (DWT, SWT, WP, GT)

The detail subimages contain the textural information in horizontal, vertical, and diagonal orientations. The approximation subimages were not used for texture analysis because they are the rough estimate of the original image and capture the intensity variations induced by lighting. The total number of sub-images or three levels of decomposition, including only the detail images, was
- 9 in the case of DWT
- 9 in the case of SWT
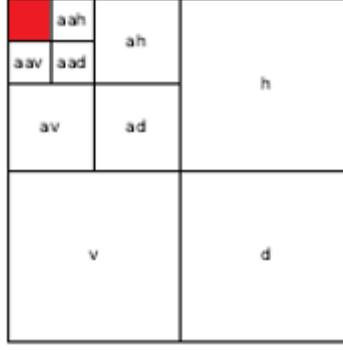- 63 in the case of WP
- 12 in the case of GT

Figure D-2 Multiresolution Feature Extraction: Ignore red sub-image

For the GT, the lowest and the highest center frequencies were set to 0.05 and 0.4, respectively. The size of the Gabor filter used for texture feature extraction was 13×13. Gabor texture information was obtained at $0, 45, 90, 135^o$.

The texture features that were estimated from each detail subimage were the mean and standard deviation of the absolute value of detail subimages, both commonly used as texture descriptors:

$$\mu_j = \frac{1}{N_1 \times N_2} \sum_{x=0}^{N_1-1} \sum_{y=0}^{N_2-1} |D_j(x,y)|$$

$$\sigma_j = \frac{1}{N_1 \times N_2} \sum_{x=0}^{N_1-1} \sum_{y=0}^{N_2-1} |D_j(x,y) - \mu_j|^2$$

where $D_j(x,y)$ are the detail sub-images of dimension $N_1 \times N_2$ in every orientation at level $j = 1,2,3$.

D.6 Amplitude Modulation-Frequency Modulation (AM-FM)

We consider multi-scale AM-FM representations, under least-square approximations, for images given by

$$f(x,y) = \sum_{n=0}^{M-1} a_n(x,y) cos\varphi_n(x,y)$$

where $n = 0,1,...,M-1$ denote different scales, $a_n(x,y)$ denotes the instantaneous amplitude (IA) for the n-th AM component, and $\varphi_n(x,y)$ denotes the instantaneous phase (IP) for the n-th FM component. In addition, the gradient of the phase $\nabla\varphi_n(x,y)$ defined as

$$\nabla\varphi_n(x,y) = \begin{bmatrix} \frac{\partial\varphi_n}{\partial x}(x,y) \\ \frac{\partial\varphi_n}{\partial y}(x,y) \end{bmatrix}$$

represents the instantaneous frequency (IF) for the n-th FM component.

Given the input discrete image $f(x,y)$, we first apply the Hilbert transform to form a $2D$ extension of the $1D$ analytic signal: $f_{AS}(x,y)$. $f_{AS}(x,y)$ is processed through a collection of bandpass filters with the desired scale. Each processing block will produce the instantaneous amplitude, the instantaneous phase, and the instantaneous frequencies in

both x and y directions. Figure below depicts the basic AM-FM demodulation method approach.
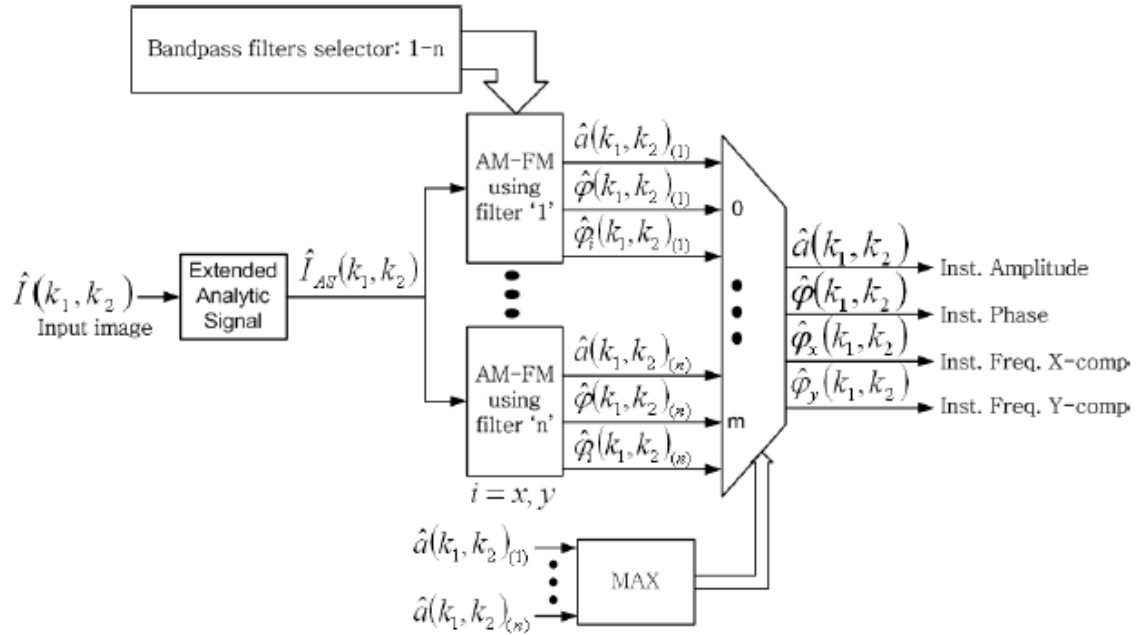

Figure D-3 2D Multi-scale AM-FM demodulation. Dominant AM-FM components are selected over different image scales. The bandpass filter selector (upper left) is used to define the bandpas filters that correspond to each scale.

As feature vector, the histogram of the low, medium, high and dc reconstructed images is used with 32 bins as a probability density function of the image.

Appendix E.   Other Features

E.1   Zernikes' Moments

Zernike moments are used to describe the shape of an object; however, since the Zernike polynomials are orthogonal to each other, there is no redundancy of information between the moments.

One caveat to look out for when utilizing Zernike moments for shape description is the scaling and translation of the object in the image. Depending on where the image is translated in the image, your Zernike moments will be drastically different. Similarly, depending on how large or small (i.e. how your object is scaled) in the image, your Zernike moments will not be identical. However, the magnitudes of the Zernike moments are independent of the rotation of the object, which is an extremely nice property when working with shape descriptors.

We can resize the object to a constant $N_1 \times N_2$ pixels, obtaining scale invariance. From there, it is straightforward to apply Zernike moments to characterize the shape of the object.

E.2   Hu's Moments

Hu Moments are used to describe, characterize, and quantify the shape of an object in an image. They are normally extracted from the silhouette or outline of an object in an image. By describing the silhouette or outline of an object, we are able to extract a shape feature vector (i.e. a list of numbers) to represent the shape of the object.

E.3   Threshold Adjacency Statistis (TAS)

Threshold adjacency statistics are generated by first applying a threshold to the image to create a binary image with a threshold chosen as follows. The average intensity, μ, of those pixels with intensity at least 30 is calculated for the image, the cut off 30 chosen as intensities below this value are in general background. The experimental image is then binary thresholded to the range $\mu - 30$ to $\mu + 30$. The range was selected to maximise the visual difference of threshold images for which the localisation images had distinct localisations but were visually similar, as in Figure 1. The following nine statistics were designed to exploit the dissimilarity seen in the threshold images. For each white pixel, the number of adjacent white pixels is counted. The first threshold statistic is then the number of white pixels with no white neighbours; the second is the number with one white neighbour, and so forth up to the maximum of eight. The nine statistics are normalised by dividing each by the total number of white pixels in the threshold image. Two other sets of threshold adjacency statistics are also calculated as above, but for binary threshold images with pixels in the ranges $\mu - 30$ to 255 and μ to 255, giving in total 27 statistics.

Bibliography

[1] Haralick, Textural Features for Image Classification

[2] Weszka, A Comparative Study of Texture Measures for Terrain Classificataion

[9] Amadasun, Texural Features Corresponding to Textural Properties

[4] Wu, Statistical Feature Matrix for Texture Analysis

[5] Wu, Texture Features for Classification

[6] Gallowway, Texture Analysis using Gray Level Run Lengths

[7] Maragos, Pattern Spectrum and Multiscale Shape Representation

[8] Toet, A hierarchical morphological image decomposition

[9] Maragos, Threshold Superposition in Morphological Image Analysis Systems

[10] Chua, Automatic indentification of epilepsy by hos and power spectrum parameters using eeg signals

[11] Chua, Application of Higher Order Spectra to Identify Epileptic eeg

[12] Acharya, Automatic identification of epileptic eeg singal susing nonlinear parameters

[13] Acharya, Application of higher order spectra for the identification of diabetes retinopathy stages

[14] Ojala, A Comparative Study of Texture Measures with Classification on Feature Distributions

[15] Ojala, Gray Scale and Roation Invariaant Texture Classification with Local Binary Patterns

[16] Murray, An AM-FM model for Motion Estimation in Atherosclerotic Plaque Videos

[17] Murray, Multiscale AMFM Demodulation and Image Reconstruction methods with Improved Accuracy

[18] Hamilton, Fast automated cell phenotype image classification

[19] Teague, Image analysis via the general theory of moments

[20] Hu, Visual Pattern Recognition by Moment Invariants

[21] Thibault, Texture Indexes and Gray Level Size Zone Matrix Application to Cell Nuclei Classification

[22] Pattichis, Medical Image Analysis Using AM-FM Models and Methods

[23] Wu, The Multi-Dimensional Ensemble Empirical Mode Decomposition Method